Energetics of Intersubunit and Intrasubunit Interactions of *Escherichia coli* Adenosine Cyclic 3′,5′-Phosphate Receptor Protein†

Xiaodong Cheng, Melva L. Gonzalez, and James C. Lee*

Department of Human Biological Chemistry and Genetics, University of Texas Medical Branch at Galveston, Galveston, Texas 77550

Received March 1, 1993; Revised Manuscript Received May 20, 1993

ABSTRACT: *Escherichia coli* cAMP receptor protein (CRP) regulates the expression of a large number of catabolite-sensitive genes. The mechanism of CRP regulation most likely involves communication between subunits and domains. A specific message, such as the activation of CRP, may be manifested as a change in the interactions between these structural entities. Hence, the elucidation of the regulatory mechanism would require a quantitative evaluation of the energetics involved in these interactions. Thus, a study was initiated to define the conditions for reversible denaturation of CRP and to quantitatively assess the energetics involved in the intra- and intersubunit interactions in CRP. The denaturation of CRP was induced by guanidine hydrochloride. The equilibrium unfolding reaction of CRP was monitored by three spectroscopic techniques, namely, fluorescence intensity, fluorescence anisotropy, and circular dichroism. The spectroscopic data implied that CRP unfolds in a single cooperative transition. Sedimentation equilibrium data showed that CRP is dissociated into its monomeric state in high concentrations of denaturant. Unfolding of CRP is completely reversible, as indicated by fluorescence and circular dichroism measurements, and sedimentation data indicated that a dimeric structure of CRP was recovered. The functional and other structural properties of renatured and native CRP have also been examined. Quantitatively identical results were obtained. Results from additional studies as a function of protein concentration and from computer simulation demonstrated that the denaturation of CRP induced by guanidine hydrochloride proceeds according to the following pathway: $(CRP_2)_{Native} \rightleftarrows 2(CRP)_{Native} \rightleftarrows 2(CRP)_{Denatured}$. The ΔG values for dissociation (ΔG_d) and unfolding (ΔG_u) in the absence of guanidine hydrochloride were determined by linear extrapolation, yielding values of 12.0 ± 0.6 and 7.2 ± 0.1 kcal/mol, respectively. To examine the effect of the DNA binding domain on the stability of the cAMP binding domain, two proteolytically resistant cAMP binding cores were prepared from CRP in the presence of cAMP by subtilisin and chymotrypsin digestion, yielding S-CRP and CH-CRP, respectively. Results from an equilibrium denaturation study indicated that the denaturation of both CH-CRP and S-CRP is also completely reversible. Both S-CRP and CH-CRP exist as stable dimers with similar ΔG_d values of 10.1 ± 0.4 and 9.5 ± 0.4 kcal/mol, respectively. Results from this study in conjunction with crystallographic data [McKay, D. B., Weber, I. T., & Stietz, T. A. (1982) *J. Biol. Chem. 257*, 9518–9524] indicate that the DNA binding domain and the C-helix are not the only structural elements that are responsible for subunit dimerization. ΔG_u for both S-CRP and CH-CRP is about 8.7 ± 0.4 kcal/mol, which is about 1.5 kcal/mol more positive than that of CRP. This implies that the isolated cAMP binding domain is more stable than the whole CRP subunit which contains both the DNA and the cAMP binding domain. These results can only be observed if there is interaction between these domains.

Escherichia coli cAMP receptor protein (CRP)[1] is a regulatory protein that acts as either a positive or a negative effector for the expression of some catabolite-sensitive genes (Zubay et al., 1970; Tsugita et al., 1982; de Crombrugghe et al., 1984). It is a dimer of two identical subunits, each of which has a molecular weight of 23 000 (Aiba et al., 1982). Each subunit consists of two domains, namely, the cAMP binding and the DNA binding domains (McKay et al., 1982; Schultz et al., 1991). Although the two binding sites for cAMP seem to be identical, the binding isotherm exhibits definite negative cooperativity (Takahashi et al., 1980; Heyduk & Lee, 1989). The binding of cAMP to CRP elicits conformational changes, which have been detected through different techniques (Wu et al., 1974; Krakow, 1975; Heyduk & Lee, 1989; Sixl et al., 1990), and could be summarized as reflecting the presence of three different states: CRP, CRP–cAMP, and CRP–$(cAMP)_2$ (Heyduk & Lee, 1989). The ability of CRP to bind specific DNA promoters is dependent on cAMP concentration (Fried & Crothers, 1984). Without cAMP only weaker nonspecific DNA binding is observed (Hudson et al., 1990), and the binding of CRP–cAMP and CRP–$(cAMP)_2$ complexes to specific DNA has been shown to be quantitatively different (Heyduk & Lee, 1989, 1990). The association constant for the DNA–CRP–cAMP complex formation is at least 80-fold higher than that for the DNA–CRP–$(cAMP)_2$ complex. The biological significance of this difference is yet to be resolved. Nevertheless, from a structural viewpoint, the activation of CRP by the binding of a single cAMP molecule must involve communication between subunits and domains.

One of the many possible approaches to elucidate the mechanism of CRP regulation is to provide a quantitative

† This work was supported by Public Service Grants DK-21489 and GM-45579 and the Robert A. Welch Foundation.

* To whom correspondence should be addressed.

[1] Abbreviations: CRP, cyclic AMP receptor protein; α-CRP, S-CRP, and CH-CRP, cAMP binding domains generated from CRP by proteolytic, subtilisin, and chymotrypsin digestion, respectively; GuHCl, guanidine hydrochloride; ANS, 8-anilino-1-naphthalenesulfonic acid; SDS, sodium dodecyl sulfate; PMSF, phenylmethanesulfonyl fluoride; DTT, dithiothreitol; Buffer A, 50 mM Tris-HCl, 0.1 M KCl, and 1 mM EDTA, pH 7.9.

0006-2960/93/0432-8130$04.00/0

evaluation of the cooperative energetics of domain–domain interactions within the same subunit and between subunits. Protein dissociation and unfolding studies can provide information on cooperative interactions between domain structures as well as subunit interactions in proteins (Bowei & Sauer, 1989; Liang & Terwilliger, 1991). This approach was employed in the present study to investigate the energetics of subunit dimerization and unfolding in CRP and the cAMP binding domain. In addition, the basic behavior of the renatured CRP and cAMP binding domain was rigorously tested to ensure the structural and functional integrity of the renatured protein.

MATERIALS AND METHODS

Materials

Glycerol, Tris, EDTA (tetrasodium salt), cAMP, subtilisin (protease type XXVII), and phenylmethanesulfonyl fluoride were purchased from Sigma. Ultrapure grade guanidine HCl was from ICN Biochemicals. Chymotrypsin A, acrylamide, and DTT were obtained from Boehringer Mannheim. ANS (Kodak Lab) was purified as described by York et al. (1978) before use. [^{3}H]cAMP and [γ-^{32}P]ATP were from Amersham, while Bio-Rex 70 was a product of Bio-Rad.

Methods

CRP was purified to homogeneity as described previously (Heyduk & Lee, 1989) and stored frozen at −20 °C in a buffer containing 50 mM Tris-HCl (pH 7.85), 20 mM KCl, 1 mM EDTA, 1 mM DTT, and 10% glycerol. Before use, CRP was thawed; dialyzed overnight, unless otherwise specified, against 50 mM Tris-HCl, 0.1 M KCl, and 1 mM EDTA, pH 7.9 (buffer A); and then filtered through a microporous filter (0.45 μm, Millipore).

S-CRP and CH-CRP were prepared from purified CRP by subtilisin and chymotrypsin digestion, respectively, in the presence of 100–200 μM cAMP at 25 °C by a procedure similar to Tsugita et al. (1982). After digestion, the proteins were purified on a Bio-Rex 70 column by a procedure based on that of Heyduk et al. (1992a). Removal of any remaining trace of cAMP bound to the proteins was achieved by dialysis and ascertained from the value of the absorbance ratio A_{280}/A_{260}. The purity of α-CRPs was examined by SDS–polyacrylamide gel electrophoresis.

For concentration determinations, the following absorption coefficients were used: 14 650 M^{-1} cm^{-1} at 259 nm for cAMP (*Merck Index*, 1976); 6240 M^{-1} cm^{-1} at 351 nm for ANS (Fergusson et al., 1975); 20 400 M^{-1} cm^{-1} at 278 nm for CRP monomer (Takahaski et al., 1980); 18 500 M^{-1} cm^{-1} at 278 nm for S–CRP and CH–CRP monomer (Gill & von Hippel, 1990).

Denaturation of CRP by GuHCl. Studies of GuHCl-induced denaturation of CRP were carried out in buffer A at 20 °C. Stock solutions of GuHCl (about 7 M) in buffer A were prepared and filtered through a 0.45-μm filter at least twice to remove any undissolved impurities. The final concentrations of the stock GuHCl solutions were determined by their densities measured with a precision DMA-02D density meter according to Kawahara and Tanford (1966). In a typical set of denaturation experiments, 20 samples of a fixed amount of CRP (final concentration of 0.20–20 μM) in buffer A were mixed with varying amounts of stock GuHCl solution to final GuHCl concentrations ranging from 0 to 6 M. Samples were equilibrated at 20 °C for at least 1 h, a period of time more than sufficient for the CRP denaturation reaction to reach equilibrium. The denaturation was monitored by fluorescence and circular dichroism.

Fluorescence measurements were made with an SLM 8000 spectrofluorometer at 20 °C. The emission spectra were recorded from 300 to 400 nm in 0.5-nm wavelength increments with an excitation wavelength of 280 nm. The spectrum of each sample was corrected by subtraction of the buffer alone. When anisotropy measurements were involved, the excitation and emission wavelengths were 280 and 345 nm, respectively.

Circular dichroism measurements were performed by using an Aviv Model 60 DS spectropolarimeter. CD spectra were measured over the range of 200–300 nm by using a 0.100- or 1.00-cm-path-length cell and protein solutions of approximately 0.1–1 mg/mL. Each spectrum was recorded in 0.5-nm wavelength increments, and the signal was acquired for 1 s at each wavelength. For each sample at least two repetitive scans were obtained and averaged.

Renaturation of CRP. After 1 h of incubation in 5 M GuHCl at room temperature, the renaturation reaction of CRP was initiated by diluting the sample to a final concentration of 2 M GuHCl. The sample was allowed to equilibrate at room temperature for another hour. The GuHCl was finally removed from the sample by extensively dialyzing the reaction mixture against buffer A at 4 °C.

Sedimentation Equilibrium. In order to provide information on the quaternary structure of CRP, the molecular weights of CRP at different GuHCl concentrations were determined by sedimentation equilibrium. A double-sector Kel-F coated 12-mm centerpiece and sapphire windows were used in a Beckman-Spinco Model E analytical ultracentrifuge equipped with a photoelectric scanner, an electronic speed control, and an RTIC temperature control. The high-speed, meniscus-depletion procedure was employed (Yphantis, 1964). The procedure for testing for attainment of equilibrium was the same as described by Schachman and Edelstein (1966). The apparent weight-average molecular weights were calculated with the following equation:

$$M_{w,app} = \frac{2RT}{(1-\bar{v}\rho)\omega^2}\frac{d(\ln c)}{dr^2} \quad (1)$$

where ω is the angular velocity, ρ is the density of solvent, c is solute concentration, r is the radial distance, $\bar{v}$ is the partial specific volume of CRP, and R and T are the gas constant and the temperature in Kelvin, respectively. Density of the solvent was determined at 20 °C with a Precision DMA-02D density meter (Mettler-Paar). The value of $\bar{v}$ of CRP in Tris buffer was calculated using the method of Cohn and Edsall (1943) on the basis of the amino acid composition of CRP (Aiba et al., 1982; Cossart & Giquel-Sanzey, 1982). The apparent partial specific volumes of CRP and α-CRP in 6.0 M GuHCl were calculated using the procedure of Lee and Timasheff (1979).

Analysis of the Denaturation Data. A three-state model is used to describe the denaturation equilibrium of CRP:

$$N_2 \overset{K_d}{\rightleftarrows} 2N \overset{K_u}{\rightleftarrows} 2U \quad (2)$$

in which N_2, N, and U are folded dimer, folded monomer, and unfolded monomer of CRP, respectively. The equilibrium constants of dissociation (K_d) and unfolding (K_u) were related to the fraction of CRP in folded states (f_1), the fraction of CRP in the folded dimer state (f_2), and the initial CRP dimer

concentration (p) in units of mol/L by

$$K_d = \frac{[N]^2}{[N_2]} = 2P\frac{(f_1 + f_1 f_2 - 2f_2)^2}{(1 + f_2)f_1} \quad (3)$$

$$K_u = \frac{[U]}{[N]} = \frac{(1 + f_2)(1 - f_1)}{f_1 + f_1 f_2 - 2f_2} \quad (4)$$

where $f_1 = (2[N_2] + [N])/(2[N_2] + [N] + [U])$ and $f_2 = [N_2]/([N_2] + [N] + [U])$. The rationale for adopting this three-state model will be addressed in the Discussion.

If the various equilibrium constants are known, the change in free energy associated with these reactions can be calculated, since

$$\Delta G_d = -RT \ln K_d \quad (5)$$

$$\Delta G_u = -RT \ln K_u \quad (6)$$

where ΔG_d and ΔG_u are the free energy changes upon dissociation and unfolding, R is the gas constant, and T is the absolute temperature.

To determine the change of free energy upon dissociation and unfolding, the fraction of CRP protein that is in the folded states (f_1) was assumed to be proportional to its measured spectroscopic signals by

$$f_1 = (\epsilon - \epsilon_{unfolded})/(\epsilon_{folded} - \epsilon_{unfolded}) \quad (7)$$

where ϵ, ϵ_{folded}, and $\epsilon_{unfolded}$ represent the measured signal of the protein sample and the signals of folded and unfolded CRP at a given GuHCl concentration, respectively. The fraction of CRP that is in the folded dimer state (f_2) was calculated from the measured apparent weight average molecular weights of CRP at different GuHCl concentration by

$$f_2 = \frac{M_{w,app} - M_m}{M_d + M_m - M_{w,app}} \quad (8)$$

where $M_{w,app}$, M_m, and M_d are the measured apparent weight average molecular weight and the molecular weights of CRP monomer and dimer, respectively. By applying $M_d = 46\,000$ and $M_m = 23\,000$ to the equation, it can be further simplified to

$$f_2 = \frac{M_{w,app} - 23\,000}{69\,000 - M_{w,app}} \quad (9)$$

Once f_1 and f_2 were determined, the data points ΔG_d and ΔG_u at different GuHCl concentrations were then fitted by a linear least-squares program to the equations

$$\Delta G_d = \Delta G_d^\circ + m_d[\text{GuHCl}] \quad (10)$$

$$\Delta G_u = \Delta G_u^\circ + m_u[\text{GuHCl}] \quad (11)$$

where ΔG_d° and ΔG_u° are the extrapolated dissociation and unfolding free energy changes of CRP in the absence of denaturant, respectively.

Analytical Gel Chromatography. The hydrodynamic properties of native and renatured CRP were also monitored by analytical gel chromatography using a procedure developed in this laboratory (Heyduk et al., 1992b). Briefly, protein samples in Tris buffer at pH 7.8 were filtered through a 1.0 × 40-cm column of Sephacryl HR 200 (Pharmacia). The column eluent was monitored by fluorescence. The flow rate was controlled by a peristaltic pump at a rate of 18.2 mL/h. The data were analyzed in accordance with eq 12,

$$K_{av} = \frac{V_e - V_o}{V_t - V_o} \quad (12)$$

where V_e, V_t, and V_o are the elution volume of the sample, the total volume, and the void volume of the column, respectively. V_o and V_t were determined by the elution volume of Blue Dextran-2000 and tryptophan amide, respectively.

Equilibrium Dialysis. cAMP binding to the native and the renatured CRP was monitored by the method of equilibrium dialysis using the previously published procedure of Heyduk and Lee (1989). Briefly, 90 μL of CRP solution at pH 7.8 and 23 °C was placed in one compartment of the cell, and 300 μL of [^{3}H]cAMP solution was placed in the other. Dialysis was conducted for 14–18 h at room temperature with continuous agitation. When equilibrium was reached, 50 μL of solution from each compartment was withdrawn, mixed with Ready-Safe scintillation cocktail (Beckman), and counted in a Beckman LS1701 scintillation counter.

Proteolytic Digestion Study. Upon binding of cAMP, CRP undergoes a structural change leading to a change in its susceptibility to proteolytic digestion (Eilen et al., 1978; Heyduk & Lee, 1989). Thus, chymotrypsin digestion was employed as a means to monitor structural change in CRP induced by cAMP binding. Proteolytic digestion was conducted in a reaction volume of 50 μL containing 0.4 mg/mL CRP and 4.8 μg/mL chymotrypsin for 80 min at 25 °C in buffer A (except 0.1 M KCl was replaced by 0.1 M NaCl) at different cAMP concentrations. Reaction was stopped by adding 0.5 μL of 100 mM PMSF in 2-propanol to a final concentration of 1 mM. Ten-microliter aliquots of the reaction mixture were withdrawn and loaded onto a 15% SDS–PAGE slab gel for analysis using a Bio-Rad Mini Protean II electrophoresis system. The gels were stained with Coomassie Blue G-200.

Binding of CRP to DNA. The wild-type *lac* promoter region was isolated from plasmid pRZ4006 using the previously published procedure (Heyduk & Lee, 1989). The fragment was labeled with ^{32}P using the kinase exchange reaction and [γ-^{32}P]ATP (Beckner & Folk, 1977; Maniatis et al., 1982). The DNA binding study was initiated by incubating different concentrations of CRP ranging from 14 to 150 nM with a fixed concentration of 100 μM or 10 mM cAMP for 30 min at room temperature. To the reaction mixture was added 2 μL of labeled DNA to a final concentration of about 20 nM in a final volume of 10 μL. Reaction was carried out for 60 min at room temperature. After equilibration, 3 μL of 15% Ficoll with tracking dye was added to the samples, which were loaded onto a 7.5% polyacrylamide gel in TBE buffer (0.09 M Tris, 0.09 M borate, and 0.0025 M EDTA) at pH 8.3. Electrophoresis was conducted at 150 V in TBE buffer containing the same concentration of cAMP as was in the binding assay. Gels were dried carefully and subjected to autoradiography using Kodak X-OMAT AR5 film.

Titration of α-CRP–ANS Complexes with cAMP. To examine the functional properties of renatured α-CRP, cAMP binding to α-CRP and renatured α-CRP was monitored by fluorescence intensity change of the α-CRP–ANS complex titrated with cAMP (Heyduk & Lee, 1989). Binding of cAMP to the α-CRP–ANS complex was studied by adding 1–2 μL of a concentrated cAMP solution (1–6 mM) to a 220-μL reaction mixture containing 9 μM α-CRP and 28 μM ANS in buffer A. The sample was excited at 360 nm, and the emission intensity was recorded at 480 nm for 2 min in 2-s increments. For each addition of cAMP, the data points were

averaged and corrected for fluorescence of free ANS by performing a parallel titration with cAMP of the sample containing ANS alone without α-CRP.

RESULTS

CRP Denaturation. Three spectroscopic methods, namely, fluorescence emission intensity at 345 nm, anisotropy, and CD absorption at 222 nm, were used to monitor the denaturation of CRP. Figure 1A shows the denaturation profile of a 22 μM solution of CRP as a function of denaturant concentrations. All three measured signals have the appearance of a cooperative transition, centered about 3 M GuHCl. The denaturation data were analyzed and expressed as the fraction of folded CRP (f_1) as a function of denaturant concentration using eq 7. Values of ϵ_{folded} and $\epsilon_{unfolded}$ at different GuHCl concentrations were obtained by extrapolating the linear portion of the denaturation curve at high and low denaturant concentration into the transition zone, as shown in Figure 1A. Figure 1B shows that the unfolding reaction follows a single and coincident transition when monitored by changes in CD, anisotropy, and fluorescence intensity. This suggests that either CD and fluorescence respond in an equivalent manner to the various species of unfolding, and the difference between the measured spectroscopic signals of folded dimer and folded monomer is very small, or only two states are significantly populated in the denaturation transition zone.

In order to identify the physical states of CRP in different GuHCl concentrations, the molecular weight of CRP was determined by sedimentation equilibrium. In native buffer and at the protein concentration used in this work, the apparent molecular weight of CRP is 46 000. Since the subunit molecular weight of CRP is 23 000, CRP must assume a dimeric structure in this experimental condition. However, in the presence of high concentrations of GuHCl, the observed molecular weight of CRP was 22 000, as shown in Figure 2. Thus, the overall unfolding reaction of CRP must start with the folded dimer and end with two unfolded monomers. In the presence of intermediary concentrations of denaturant, the sedimentation data yielded $M_{w,app}$ values that are between 46 000 and 22 000, suggesting that in the pre-denaturation transition zone, i.e., at about 2 M GuHCl, significant amounts of monomer and dimer are present. The fractions of folded states (f_1) and folded dimer states (f_2) can be obtained from the spectroscopic and sedimentation measurements, respectively, by applying eqs 7 and 9, as shown in Figure 3A. The values of f_1 and f_2 having been determined, it is possible to calculate K_d and K_u in accordance with eqs 3 and 4. Furthermore, the corresponding values of ΔG can be calculated. By assuming a linear relationship between ΔG and denaturant concentration, ΔG_d° and ΔG_u° in the absence of denaturant can be estimated by using eqs 10 and 11. For CRP, the free energy changes for dimer dissociation and monomer unfolding in the absence of denaturant were 12.0 $\pm$ 0.6 and 7.2 $\pm$ 0.1 kcal/mol, respectively, as shown in Figure 3B.

In order to identify the specific mechanism of the denaturation reaction of a dimeric protein, the denaturation reaction was monitored as a function of protein concentration. An additional denaturation study was conducted with a 1 μM solution of CRP, and the results are shown in Figure 1C. There is a significant protein concentration dependence in the transition curves as GuHCl concentrations between 2 and 3 M but a much smaller dependence at GuHCl concentrations higher than 3 M. Using the three-state model as described in Methods, the denaturation curves at different CRP

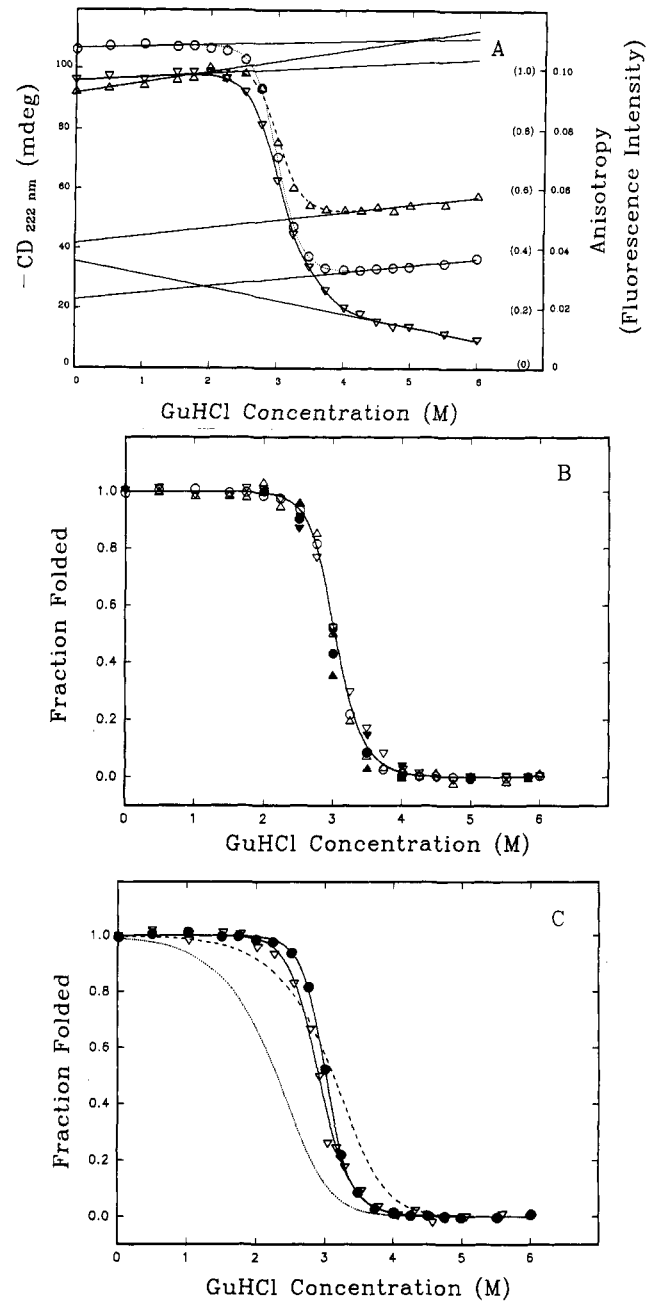

FIGURE 1: Unfolding of CRP by GuHCl monitored by spectroscopic methods. (A) The denaturation was carried out in 50 mM Tris-HCl, 100 mM KCl, 1 mM EDTA, and 1 mM DTT, pH 7.9, by exposing CRP (22 μM) to different concentrations of GuHCl. After 1 h of equilibration at 20 °C, the unfolding reaction was monitored by changes in anisotropy (○), fluorescence intensity at 345 nm (△), and circular dichroism at 222 nm (▽). (B) Estimates of fractions of CRP in the folded states determined by using anisotropy (○), fluorescence intensity (△), and $CD_{222\ nm}$ (▽). The filled symbols represent data that were measured after CRP was first equilibrated in buffer A containing 6 M GuHCl and then diluted to the indicated GuHCl concentrations and equilibrated for at least another hour. The refolding reaction was monitored by circular dichroism (▼), fluorescence intensity (▲), and anisotropy (●) with 9 μM CRP. (C) Dependence of CRP denaturation on protein concentration. Anisotropy values at 1 (▽) and 22 μM CRP (●) were measured as a function of GuHCl concentration at 20 °C. The solid lines are the theoretical curves calculated according to a three-state model using the parameters obtained from Figure 3. The long dash line (– –) is the best fit of the data at 22 μM CRP to a two-state model (eq 19), and the short dash line (- - -) is the predicted curve for CRP denaturation at 1 μM protein concentration using the parameters derived from the best fit using the same model.

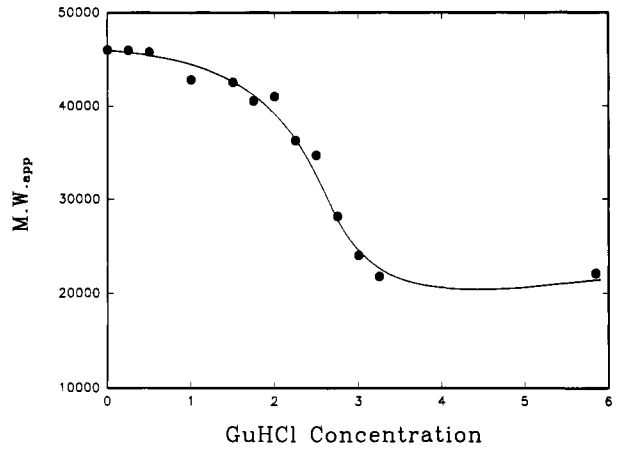

FIGURE 2: Apparent weight average molecular weight of CRP as a function of GuHCl concentration. Sedimentation equilibrium data were collected in 50 mM Tris, pH 7.9, 100 mM KCl, and 1 mM EDTA at 20 °C.

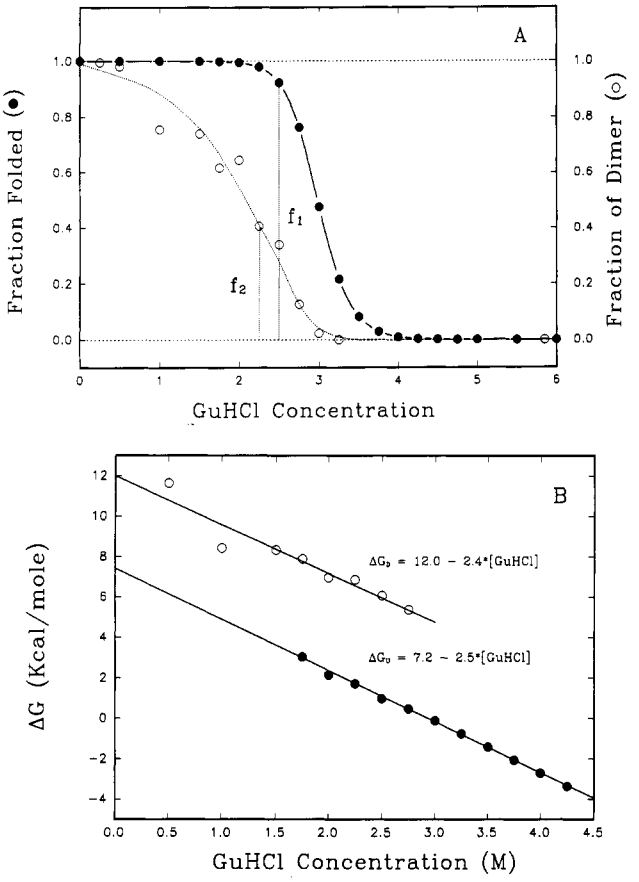

FIGURE 3: (A) Fraction of CRP in folded states (f_1) monitored by a spectroscopic technique (●), and fraction of CRP in dimer (f_2) monitored by sedimentation equilibrium (○), as a function of GuHCl concentrations. (B) Free energy for unfolding (ΔG_u) and dissociation (ΔG_D) of CRP as a function of GuHCl concentration.

concentrations can be predicted since

$$f_1 = \{8[\mathrm{CRP}] + K_d K_u(1 + K_u) - K_u[(K_d + K_d K_u)^2 + 16[\mathrm{CRP}]K_d]^{1/2}\}/8[\mathrm{CRP}] \quad (13)$$

with $K_d = K_d^\circ \exp - m_d[\mathrm{GuHCl}]/RT$ and $K_u = K_u^\circ \exp - m_u[\mathrm{GuHCl}]/RT$. The parameters used for this simulation were the values derived from least-squares fitting in Figure 3B. As shown in Figure 1C, calculated denaturation curves fit quite well to the data points. Thus, all the data are consistent with the three-state model, and the values of ΔG_d° and ΔG_u° obtained according to eqs 10 and 11 are most likely valid estimations of the free energy changes of dissociation and unfolding of CRP.

Reversible Denaturation of CRP. The reversibility of CRP denaturation induced by GuHCl was tested. As shown in Figure 1B, the CD, fluorescence intensity, and anisotropy data are independent of the starting concentration of GuHCl, be it 0 or 6 M. The CRP protein unfolded in 6 M GuHCl can be reversibly refolded when diluted to a lower concentration of denaturant. Sedimentation equilibrium analysis suggests that renatured CRP has regained its quaternary structure and exists as a dimer just like the native CRP before exposure to GuHCl. To further test the structural integrity of renatured CRP, a sensitive analytical gel chromatographic procedure was employed to compare the hydrodynamic properties of the native and the renatured CRP. Large-zone experiments were conducted at an identical protein concentration of 0.48 μM in Tris buffer (50 mM Tris, 0.3 M KCl, and 1 mM EDTA at pH 7.8 and 23 °C). The elution profiles were superimposable. It is evident that the two CRP samples exhibited the same elution properties. On the basis of the elution volumes of the CRP samples, it was determined that the native and the renatured CRP both exist as a globular protein with a Stokes radius of 28.4 Å.

Because it has been determined that denatured CRP can be reversibly renatured into a state that exhibits the same gross physical properties as the native protein, it is important to test for reversibility of the functional properties. Hence, the renatured CRP was subjected to three rigorous quantitative tests, namely, its ability to bind cAMP, the effect of low and high concentrations of cAMP on the structure of CRP, and its ability to bind to the *lac* promoter.

cAMP binding to native and renatured CRP was monitored by equilibrium dialysis. The binding data were collected for free cAMP concentrations below 200 μM only, i.e., under conditions where CRP–cAMP is the predominant species (Heyduk & Lee, 1989). No attempts were made to measure cAMP binding at higher cAMP concentrations because the binding of the second site exhibits negative cooperativity, and it is very difficult to obtain an accurate estimation of the association constant by direct binding experiments. The cAMP binding data for native and renatured CRP are very similar. Overlapping data points are observed throughout the whole range of cAMP concentration studied, as shown in Figure 4. To obtain the association constant for cAMP binding, the data were fitted to eq 14

$$N_s = \frac{K_1[\mathrm{cAMP}] + 2K_2[\mathrm{cAMP}]^2}{1 + K_1[\mathrm{cAMP}] + K_2[\mathrm{cAMP}]^2} \quad (14)$$

where N_s is the ratio of cAMP bound per mole of CRP dimers, [cAMP] is the concentration of free ligand, and K_1 and K_2 are the association constants of formation of CRP–cAMP and CRP–$(cAMP)_2$ complexes, respectively. In this study, K_2 is fixed at 7.6×10^7 M^{-1} (Heyduk & Lee, 1989). Equilibrium constants of $(4.6 \pm 0.4) \times 10^4$ and $(5.0 \pm 1.5) \times 10^4$ M^{-1} can be obtained for the native and the renatured CRP, respectively. Thus, it may be concluded that denatured CRP can be reversibly renatured so that one cannot distinguish the native from the renatured CRP with respect to the binding affinity of the first cAMP site.

In an earlier study, it has been demonstrated that the binding of cAMP to the first site elicits a different structural change in CRP compared to binding at the second site (Heyduk & Lee, 1989). At low cAMP concentrations ranging from 0 to 200 μM, the rate of proteolytic digestion increases, while at higher cAMP concentrations, the rate decreases. In order to

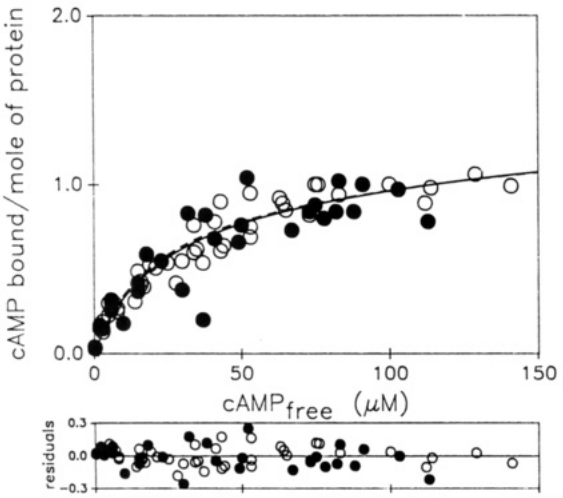

FIGURE 4: [^{3}H]cAMP binding to CRP in Tris buffer at pH 7.8 and 23 °C. The open and filled circles are data for the native and the renatured CRP, respectively. The solid and broken lines are the fitted curves using eq 14 and K_1 values of 4.6×10^4 and 5.0×10^4 M^{-1}, respectively.

test the behavior of CRP in the presence of cAMP as completely as possible, the native and the renatured CRP were subjected to chymotrypsin digestion at cAMP concentrations ranging from 0 to 50 mM. Figure 5 shows the results of chymotrypsin digestion. Under the experimental conditions employed, there is no detectable digestion of either the native or the renatured CRP in the absence of cAMP. Qualitatively, the amount of digested CRP increases with cAMP concentration for both the native and the renatured CRP, reaching a maximum at 200 μM cAMP. Upon further increases of cAMP concentration, the amount of digested CRP decreases. Essentially identical results were observed for either the native or the renatured CRP.

The functional testing of the renatured CRP has been centered around cAMP binding and the structural responses to cAMP binding. One needs to evaluate the ability of the renatured CRP in its binding to *lac* promoter. Heyduk and Lee (1989, 1990) have demonstrated quantitatively that the CRP–cAMP and CRP–$(cAMP)_2$ complexes have different affinities for the *lac* promoter. The CRP–$(cAMP)_2$ complex exhibits at least an 80-fold decrease in affinity. Thus, the binding of CRP to the *lac* promoter was monitored by gel retardation assay. An increasing amount of CRP was titrated into a solution of fixed concentrations of 100 μM cAMP and 20 nM DNA (the 203-bp fragment that contains the *lac* promoter). Under these conditions, the CRP–cAMP complex should be the predominant species. The results are summarized in Figure 6. The native CRP sample showed that the amount of protein–DNA complex increased from 57% to 94% when CRP concentration was increased from 14 to 98 nM, while for the renatured CRP the amount of complex increased from 72% to 96% when the concentration of CRP was increased from 15 to 105 nM. One may then conclude that the renatured CRP forms a protein–DNA complex with the same apparent affinity as the native protein. In order to test the affinity of the CRP–$(cAMP)_2$ complex for specific DNA, the experiment was conducted at 10 mM cAMP, at which concentration the predominant species is CRP–$(cAMP)_2$. For native CRP, the amount of protein–DNA complex detected ranged from 0% to 21% when the CRP concentration was increased from 14 to 140 nM. For the renatured CRP, the amount of complex detected varied from 4% to 20% when the CRP concentration was increased from 38 to 155 nM. Hence the renatured CRP is exhibiting the same quantitative behavior as the native CRP, i.e., the CRP–$(cAMP)_2$ complex has a much lower affinity for a specific DNA site.

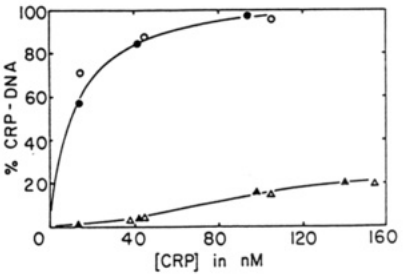

FIGURE 6: Binding of native and renatured CRP to the 203-bp fragment of *lac* promoter DNA at pH 7.8 and 23 °C in 100 μM and 10 mM cAMP concentrations using the gel retardation assay. The data are expressed in % of CRP–DNA complex as a function of CRP concentrations. The filled circles and triangles represent data for native CRP in 100 μM and 10 mM cAMP, respectively. The open circles and triangles represent data for renatured CRP in 100 μM and 10 mM cAMP, respectively. The lines were drawn to indicate the trend of the data only.

Denaturation of α-CRP. To examine the effect of the DNA binding domain on the stability of CRP, α-CRP was generated. The apparent molecular weight of S-CRP was determined by sedimentation equilibrium, and a value of 27 000 was obtained. Since the subunit molecular weight was about 13 000, S-CRP must exist as a dimer in native buffer. Denaturation of S-CRP was also conducted, and the results are summarized in Figure 7A. The apparent denaturation profile of S-CRP resembles

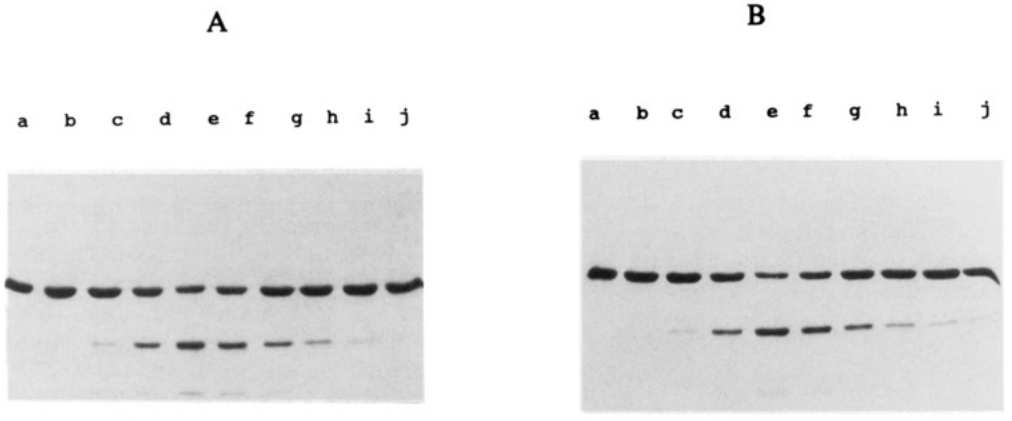

FIGURE 5: Proteolytic digestion of CRP by subtilisin at different cAMP concentrations for (A) native and (B) renatured protein. In both panels, lane a was CRP alone, and lanes b-j contained protease and different concentrations of cAMP: b, 0; c, 5 μM; d, 20 μM; e, 200 μM; f, 2 mM; g, 5 mM; h, 10 mM; i, 25 mM; j, 50 mM.

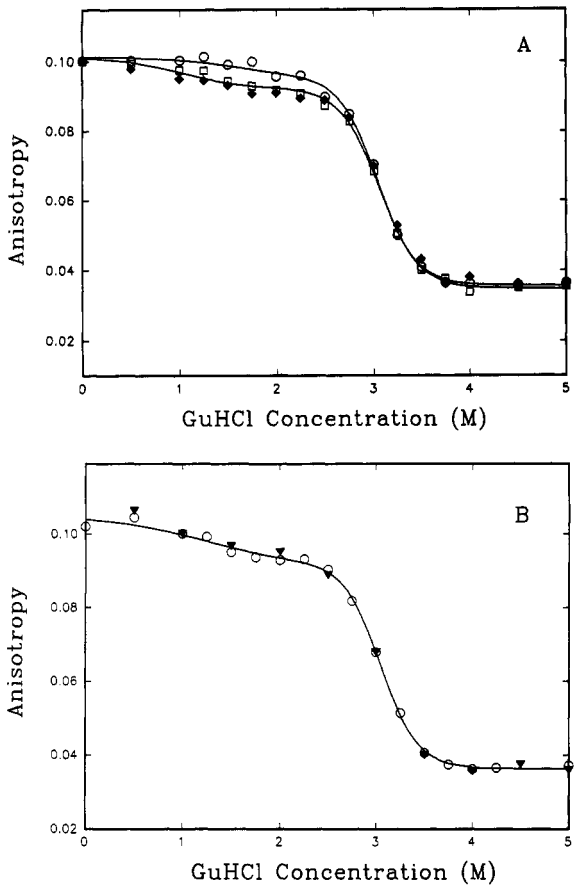

FIGURE 7: Denaturation and renaturation of α-CRP by GuHCl. (A) Denaturation of S-CRP at 13.6 (○) and 1.3 μM protein (□) and renaturation at 1.3 μM protein concentration (◆). (B) Reversible denaturation of CH-CRP monitored by anisotropy. The protein concentration was 1.5 μM in the denaturation (○) and renaturation studies (▼).

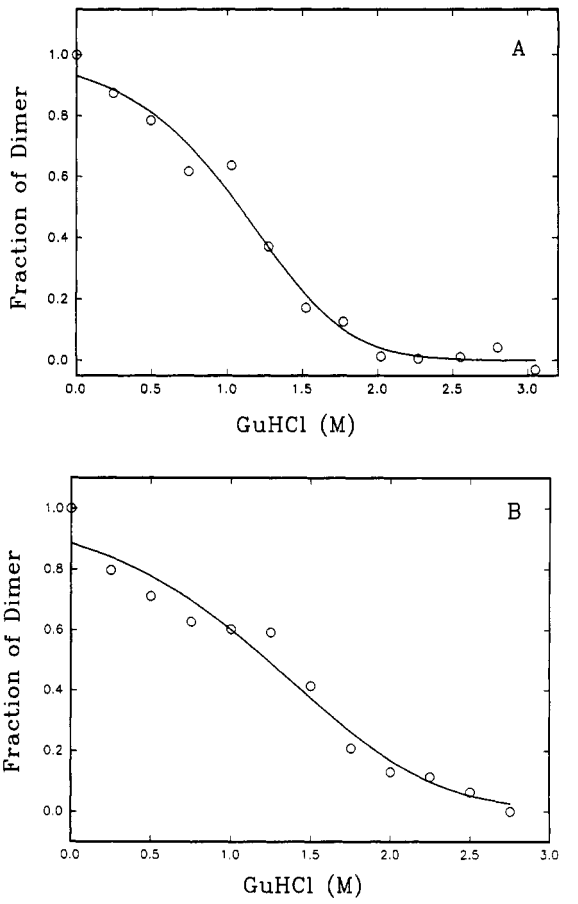

FIGURE 8: Fraction of α-CRP in dimer monitored by sedimentation equilibrium as a function of GuHCl concentration. The total protein concentration was 5.3 μM. The equilibrium dissociation constant of α-CRP was determined from the least-squares fitting of the data. (A) S-CRP, $K_d = 2.8 \times 10^{-8}$ M. (B) CH-CRP, $K_d = 8.2 \times 10^{-8}$ M.

that of CRP, although significant differences were detected. At 13.6 μM S-CRP, the denaturation curve is monophasic. However, when the S-CRP protein concentration was decreased to 1.3 μM, a biphasic denaturation profile was observed. It is interesting to note that at low GuHCl concentrations (<2.5 M) the denaturation data were dependent on protein concentration, whereas the denaturation data at high GuHCl concentrations (>3 M) were independent of S-CRP concentration. This suggests that the S-CRP denaturation followed a pathway similar to that described for CRP, i.e., dissociation of S-CRP dimer to folded monomer preceds the unfolding process.

Sedimentation equilibrium data shown in Figure 8 indicate that at 2 M GuHCl S-CRP exists as a species with a molecular weight of about 13 000, i.e., S-CRP exists as a monomer at 2 M GuHCl. This suggests that the dissociation of S-CRP is uncoupled from the unfolding event, and the apparent molecular weights of S-CRP in the presence of intermediate concentrations of GuHCl should reflect the dissociation of S-CRP. Therefore, the equilibrium constant of S-CRP dissociation can be estimated from sedimentation equilibrium data by fitting the data to equation 15, where the fraction of S-CRP in dimer is expressed as

$$f = \frac{(K_d^2 + 16PK_d)^{1/2} - K_d}{(K_d^2 + 16PK_d)^{1/2} + 3K_d} \qquad (15)$$

where P is the initial S-CRP molar concentration in dimer and K_d is the dimer dissociation constant. The value of the dissociation constant in the absence of denaturant, K_d°, is determined by nonlinear least-squares analysis by substituting K_d with $K_d^\circ \exp - m_d[\text{GuHCl}]/RT$, which assumes the dissociation free energy change is linear with GuHCl concentration. A value of $(5.3 \pm 2.7) \times 10^{-8}$ was obtained. Similarly, the equilibrium constant of S-CRP unfolding, K_u°, can also be solved by fitting the data in Figure 7A to eq 16,

$$A = \frac{A_N + A_D K_u^\circ \exp - m_u[\text{GuHCl}]/RT}{1 + K_u^\circ \exp - m_u[\text{GuHCl}]/RT} \qquad (16)$$

where A, A_N, and A_D are the measured apparent anisotropy, the anisotropy for folded S-CRP monomer, and the anisotropy for unfolded S-CRP monomer, respectively. Only data at GuHCl concentrations greater than 2.25 M which represent the unfolding reaction were used. The fitted value of the unfolding constant is $(2.9 \pm 2.5) \times 10^{-7}$.

The reversibility of the denaturation of S-CRP was tested, and the results are shown in Figure 7A. The spectroscopic data for the renaturation study are completely superimposable on the denaturation curve, indicating that the denaturation of S-CRP is completely reversible. Upon renaturation, the dimeric structure of S-CRP was restored, as indicated by the results from sedimentation equilibrium analysis.

The biological function of the renatured S-CRP was monitored. Fluorescence titration of S–CRP–ANS complex with cAMP was used to study the binding of cAMP to S-CRP, as it has been shown previously that cAMP binding quenches fluorescence of ANS by displacing it from a complex with the protein. Identical results were obtained for both S-CRP and

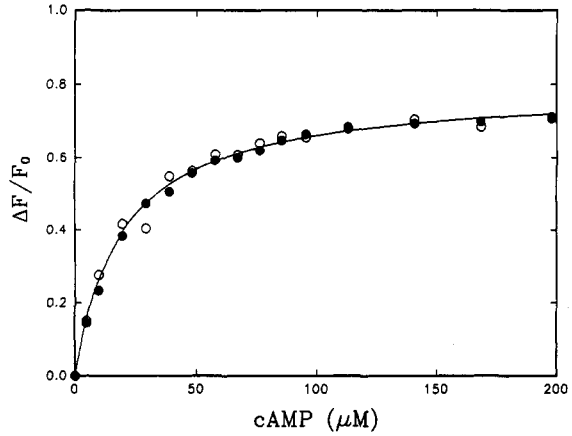

FIGURE 9: Binding of cAMP to native (○) and renatured S-CRP (●) monitored by quenching of fluorescence of the S–CRP–ANS complex. The data are expressed in percentage change of the fluorescence intensity ($\Delta F/F_0$) as a function of cAMP concentration.

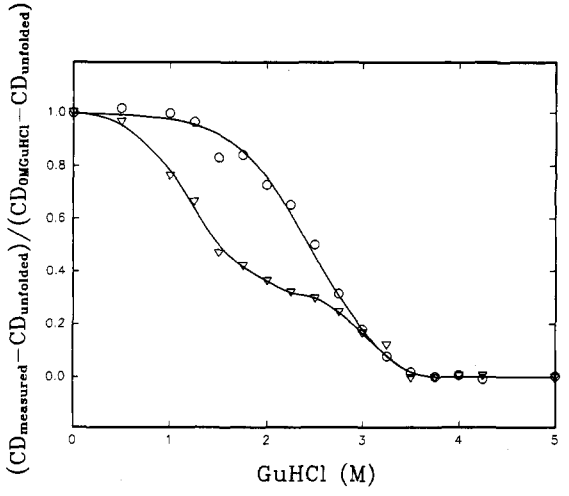

FIGURE 10: Denaturation of CH-CRP monitored by CD at 222 nm: 15 (○) and 1.5 μM CH-CRP (▽).

renatured S-CRP, as shown in Figure 9. Hence, these results show that the denaturation process of S-CRP is completely reversible both structurally and functionally.

Denaturation of CH-CRP was also studied. In Figure 7B, the anisotropy of CH-CRP was monitored as a function of GuHCl concentration. It is apparent that, unlike that of CRP, the denaturation curve of CH-CRP exhibits a profile that resembles that of S-CRP at low protein concentrations, namely, the presence of a slope in the pre-denaturation region. It is conceivable that the dissociation of CH-CRP is more uncoupled from the unfolding event. Therefore, the dissociation and unfolding constants of CH-CRP can be determined by studying the two reactions separately. The fraction of CH-CRP in dimer was calculated from the weight average molecular weight of CH-CRP determined by sedimentation equilibrium, and the results are shown in Figure 8B. It is clear that more than 90% of CH-CRP has already dissociated into the monomeric state at 2.25 M GuHCl, at which concentration CH-CRP starts to unfold. So the dimer dissociation constant of CH-CRP can be estimated by nonlinear least-squares fitting of the data in Figure 8B, using the same approach employed for S-CRP.

The denaturation of CH-CRP was also monitored by CD, as shown in Figure 10. The denaturation profile is dependent on protein concentration, while the measured fluorescence intensity is independent. These results imply that the unfolding of CH-CRP most likely proceeds in a mechanism that is more

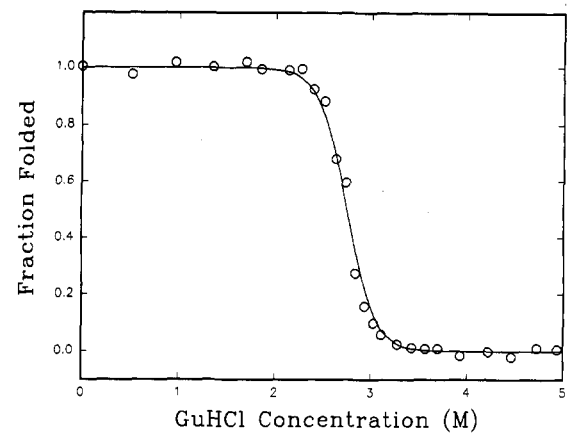

FIGURE 11: Fraction of CH-CRP in folded states determined by fluorescence intensity. The unfolding constant of CH-CRP was determined from the least-squares fitting of the data: $K_u = 3.7 \times 10^{-7}$.

complicated than a two-state concerted pathway. A close examination of the CH-CRP structure reveals that the C-helix accounts for more than 50% of the α-helix content in CH-CRP and all the aromatic amino acid residues that contribute to the protein fluorescence except one phenylalanine (Phe^{137}) are located in portions of the protein other than the C-helix. It may be concluded that dissociation of the CH-CRP dimer leads to an unfolding of the C-helix while the rest of the protein structure still remains folded in the CH-CRP monomer.

Since the denaturation of CH-CRP measured by fluorescence intensity is protein concentration independent, it can be examined more accurately by titrating the CH-CRP with GuHCl. In such a study, the equilibrium constant of the CH-CRP monomer, K_u^0, can be determined by fitting the data in Figure 11 to the equation

$$f = \frac{1}{1 + K_u^0 \exp - m_u[\text{GuHCl}]/RT} \qquad (17)$$

DISCUSSION

The basic biological function of CRP is activation of gene expression by binding to specific DNA promoters. The signal to activate CRP is the binding of cAMP. Two molecules of cAMP can bind to each dimeric molecule of CRP, although the affinity for the second cAMP is much weaker. Among the species that can bind to the *lac* promoter, the single-liganded species of CRP–cAMP has been shown to bind at least 80-fold more strongly than the CRP–$(cAMP)_2$ species to this specific DNA site. This observation indicates that the CRP activation process must involve the transmission of information, acquired by the binding of one cAMP molecule, from one subunit to another. Furthermore, the information must also have to be transmitted from the cAMP binding N-terminal domain to the DNA binding C-terminal domain. Thus, subunit–subunit and domain–domain interactions must play important roles in regulating the biological functions of CRP. Transmission of information through these interfaces may generate a change in the interfacial interactions that are amplified as a change in the energetics that define the domain–domain and subunit–subunit interactions.

In this study the energetics of these interfacial interactions are monitored by chemical denaturation. The usefulness of this study depends on the success in establishing the unfolding pathway. Hence, it is important to examine the evidence employed to support the proposed pathway. There are three possible unfolding pathways for a dimeric protein. If the CRP

Table I: Summary of Fitted Equilibrium Constants

protein	K_d° (M)	K_u°	ΔG_u (kcal/mol)
CRP	1.0×10^{-9} (4.1×10^{-10}–3.0×10^{-9})	4.2×10^{-6} (3.6×10^{-6}–5.0×10^{-6})	7.2
S-CRP	2.8×10^{-8} (1.4×10^{-8}–6.0×10^{-8})	2.9×10^{-7} (1.6×10^{-7}–4.1×10^{-7})	8.7
CH-CRP	8.2×10^{-8} (4.4×10^{-8}–1.8×10^{-7})	3.7×10^{-7} (2.8×10^{-7}–4.8×10^{-7})	

dimer dissociates before it starts unfolding, then the unfolding reaction would be a unimolecular equilibrium between folded and unfolded monomer, as expressed by eq 18. The latter

$$N_2 \overset{K_d}{\rightleftarrows} 2N$$

$$N \overset{K_u}{\rightleftarrows} U \qquad (18)$$

reaction would be independent of protein concentration. Furthermore, if CRP unfolds directly from a folded dimer into two unfolded monomers, that is,

$$N_2 \overset{K}{\rightleftarrows} 2U \qquad (19)$$

then the entire transition zone of the denaturation curve would shift as the protein concentration changes, as shown in Figure 1C. Thus, a study of CRP denaturation as a function of protein concentration should provide evidence to distinguish between these two possible pathways. Results from this study show that the denaturation of CRP by GuHCl, monitored by fluorescence intensity, anisotropy, and circular dichroism, can be represented by a single cooperative transition, indicating that the denaturation process is apparently a concerted two-state reaction. However, upon further examination of the denaturation reaction by sedimentation equilibrium analysis, the results indicate that the predenaturation zone is populated by a significant amount of both folded dimer and monomer. Hence, denaturation of CRP dimer can best be described by a three-state model, i.e., dissociation of CRP dimer is coupled with an unfolding of CRP monomer. Unfolding of the CRP monomer starts before all of the CRP dimers have been dissociated into monomers, so the equilibrium constants for dissociation and unfolding can be estimated from a detailed examination of the denaturation reaction. The validity of this model is supported by the shape of the denaturation curves as a function of protein concentration. Dissociation of CRP dimer to monomer is protein concentration dependent, whereas the unfolding of CRP monomer is not.

Denaturation of α-CRP can be represented by the same model as expressed by eq 18. The same pattern of protein concentration dependence is observed. Consequently, values for K_d and K_u can be extracted for both CRP and α-CRP leading to an insight to the effect of the DNA binding domain on the energetics of subunit–subunit interaction and the stability of these domains.

The dissociation constant for CRP, K_d, is about 1×10^{-9} M at 20 °C in 50 mM Tris-HCl (pH 7.9), 1 mM EDTA, and 100 mM KCl (Table I). This value is consistent with our previous observation that the CRP starts to dissociate around 10^{-8}–10^{-9} M protein concentration (Heyduk et al., 1992b) but is different from the value of 2.5×10^{-11} M reported by Brown and Crothers (1989). The latter study was conducted at 37 °C in 10 mM Tris-HCl (pH 8.0), 50 mM NaCl, 1 mM EDTA, 0.05% Tween-80, and 10% glycerol. The observed difference in the value of K_d reported in this study and the literature may be due to the different solvent conditions and temperature used. Glycerol is known to stabilize proteins and to enhance protein aggregation (Lee & Timasheff, 1975; Na & Timasheff, 1981). Thus, it is not surprising that the reported K_d in 10% glycerol is lower than that observed in this study.

It is interesting to note that in the absence of denaturant both S-CRP and CH-CRP are dimeric with similar stability (Table I). On the basis of the crystalline structure of CRP, most of the intersubunit interaction occurs between the two long C-helices. CH-CRP consists of amino acid residues 1–137; thus it retains the complete C-helix, and it is not surprising to note that CH-CRP does exist as a dimer. S-CRP consists of amino acid residues 1–114 and is essentially depleted of the C-helix. Yet, both α-CRP species exist as a dimer. This indicates that the C-helix is not the only structural element that is responsible for subunit dimerization. Another possible interpretation of the current observation is that removal of the C-terminal domains leads to a major reorientation of the intersubunit contacts between the N-terminal domains. The results of the cAMP binding study indicate that α-CRP can still bind cAMP with high affinity; thus, any reorientation, if it happens, cannot be major, although results from a near-UV CD study indicate that the microenvironments of the aromatic residues of the chains are perturbed when CRP is transformed to α-CRP (Blazy et al., 1992).

The unfolding of CRP is completely cooperative, with an unfolding equilibrium constant of 4.2×10^{-6}. No stable folding intermediate was detected with all the techniques employed in this study. This suggests that the DNA and cAMP binding domains in CRP respond to the denaturant in a concerted manner during the unfolding process. The unfolding of S-CRP and CH-CRP also proceeds without a stable folding intermediate as monitored by fluorescence techniques. The results show no dependence on protein concentration. However, the unfolding of CH-CRP showed significant dependence on protein concentration when the reaction was monitored by circular dichroism. The ellipticity at 222 nm changes significantly as a function of protein concentration a <3 M GuHCl. The source of the apparent discrepancy between the fluorescence and CD data can be traced to the C-helix. Because the C-helix accounts for more than 50% of the α-helical content in CH-GRP, and because almost all of the aromatic amino acid residues except one phenylalanine (phe^{137}) are located in the N-terminal domain apart from the C-helix portion, it is interpreted that the C-helix is unfolded upon dissociation of the CH-CRP dimer while the rest of the protein structure remains folded. So in the sense of structural folding, the C-helix is not a part of the N-terminal domain.

The equilibrium unfolding constant for both S-CRP and CH-CRP is about 3×10^{-7} (Table I), which is about 10-fold smaller than that of CRP. Let us examine the significance of these observations with respect to interactions between the DNA and cAMP binding domains. In a protein system with two domains, D_1 and D_2, the energetics of unfolding and their relations can be expressed as

$$D_1D_2 \overset{\Delta G_1}{\rightleftarrows} U_1D_2 \overset{\Delta G_2}{\rightleftarrows} U_1U_2 \qquad (20)$$

where U_1 and U_2 are the unfolded states of D_1 and D_2, respectively, and ΔG_1 and ΔG_2 are the ΔG's for unfolding of D_1 and D_2, respectively. The overall ΔG for unfolding of

D_1D_2 is ΔG_T. The relations among the ΔG's are

$$\Delta G_T = \Delta G_1 + \Delta G_2 + \Delta G_{12} \quad (21)$$

where ΔG_{12} is the coupling energy between the two domains. If the domains are independent of each other, then ΔG_{12} = 0 and ΔG_T is simply the summation of ΔG_1 and ΔG_2. In the context of this study, D_1 and D_2 are the DNA and cAMP binding domains of CRP, respectively. Thus, ΔG_1 and ΔG_2 are the unfolding free energy changes of the DNA and cAMP binding domains. An estimation of ΔG_2 can be taken from Table I using the values of K_u for S-CRP and CH-CRP. An average value of ΔG_2 = 8.7 kcal/mol can be calculated. Furthermore, the observed value of K_u for CRP should be an appropriate assessment of ΔG_T, and it assumes a value of 7.2 kcal/mol. From eq 21, $\Delta G_1 + \Delta G_{12}$ is −1.5 kcal/mol. If ΔG_{12} = 0, then ΔG_1 = −1.5 kcal/mol, a value which implies that the DNA binding domain is unstable and would exist in an unfolded state. However, folded CRP monomer which consists of both domains was shown to be present in low concentrations of GuHCl; thus, the DNA binding domain exists in a folded state in the presence of the cAMP binding domain, i.e., ΔG_1 is positive in the presence of D_2. This leads to an estimated value for ΔG_{12} more negative than −1.5 kcal/mol. This implies that the stability of the N-terminal domain is influenced by the presence of the C-terminal domain, and the net consequence is to destabilize the molecule. The role of destabilization in the mechanism of CRP activity is yet unknown. Studies on the effect of cAMP binding on these intersubunit and interdomain interactions should yield useful information to address this issue.

ACKNOWLEDGMENT

We thank Dr. Ewa Heyduk for her assistance in the experiments using analytical gel chromatography and Dr. Tomasz Heyduk for his continuous interest in this project.

REFERENCES

Aiba, H., Fujimoto, S., Ozaki, N. (1982) *Nucleic Acids Res. 10*, 1345–1361.
Berkner, K. L., & Folk, W. R. (1977) *J. Biol. Chem. 252*, 3176–3184.
Blazy, B., Baudras, A., & Maurizot, J. C. (1992) *Biochim. Biophys. Acta 1120*, 223–227.
Bowei, J. V., & Sauer, R. T. (1989) *Biochemistry 28*, 7139–7143.
Brown, A. H., & Crothers, D. M. (1989) *Proc. Natl. Acad. Sci. U.S.A. 86*, 7387–7391.
Cohn, E. J., & Edsall, J. T. (1943) *Proteins, Amino Acids and Peptides*, p 372, Van Nostrand-Reinhold, Princeton, NJ.
Cossazt, P., & Gicquel-Sanzey, B. (1982) *Nucleic Acids Res. 10*, 1363–1378.
de Crombrugghe, B., Busby, S., & Buc, H. (1984) *Science 224*, 831–838.
Eilen, E., Pampeno, C., & Krakow, J. S. (1978) *Biochemistry 17*, 2469–2479.
Ferguson, R. N., Edelhoch, H., Saroff, H. A., & Robbins, J. (1975) *Biochemistry 14*, 282–289.
Fried, M. G., & Crothers, D. M. (1984) *J. Mol. Biol. 172*, 241–262.
Gill, S. C., & von Hippel, P. H. (1989) *Anal. Biochem. 182*, 319–326.
Heyduk, T., & Lee, J. C. (1989) *Biochemistry 28*, 6914–6924.
Heyduk, T., & Lee, J. C. (1990) *Proc. Natl. Acad. Sci. U.S.A. 87*, 1744–1748.
Heyduk, E., Heyduk, T., & Lee, J. C. (1992a) *Biochemistry 31*, 3682–3688.
Heyduk, E., Heyduk, T., & Lee, J. C. (1992b) *J. Biol. Chem. 267*, 3200–3204.
Hudson, J. M., Crowe, L. G., & Fried, M. G. (1990) *J. Biol. Chem. 265*, 3219–3225.
Kawahara, K., & Tanford, C. (1966) *J. Biol. Chem. 241*, 3228–3232.
Krakow, J. S. (1975) *Biochim. Biophys. Acta 383*, 345–350.
Lee, J. C., & Timasheff, S. N. (1975) *Biochemistry 14*, 5183–5187.
Lee, J. C., & Timasheff, S. N. (1979) *Methods Enzymol. 61*, 49–57.
Liang, H., & Terwilliger, T. C. (1991) *Biochemistry 30*, 2772–2782.
Maniatis, T., Fritsch, E. F., & Sambrook, J. (1982) *Molecular Cloning*, Cold Spring Harbor Laboratory, Cold Spring Harbor, NY.
McKay, D. B., Weber, I. T., & Streitz, T. A. (1982) *J. Biol. Chem. 257*, 9518–9524.
Na, G. C., & Timasheff, S. N. (1981) *J. Mol. Biol. 151*, 165–178.
Schachman, H. K., & Edelstein, S. J. (1966) *Biochemistry 5*, 2681–2705.
Schultz, S. C., Shileds, G. C., & Steitz, T. A. (1991) *Science 253*, 1001–1007.
Sixl, F., King, R. W., Bracken, M., & Feeney, J. (1990) *Biochem. J. 266*, 545–552.
Takahashi, M., Blazy, B., & Baudras, A. (1980) *Biochemistry 19*, 5125–5130.
The Merck Index, (1976) 9th ed., p 353, Merck & Co., Inc., Rahway, NJ.
Tsugita, A., Blazy, B., Takahashi, M., & Buadras, A. (1982) *FEBS Lett. 144*, 304–308.
Wu, F. Y.-H., Nath, K., & Wu, C.-W. (1974) *Biochemistry 13*, 2567–2572.
York, S. S., Lawson, R. C., Jr., & Worah, D. M. (1978) *Biochemistry 17*, 4480–4486.
Yphantis, D. A. (1964) *Biochemistry 3*, 297–317.
Zubay, G., Schwartz, D., & Beckwith, J. (1970) *Proc. Natl. Acad. Sci. U.S.A. 66*, 104–110.